Journal of
Manufacturing and Materials Processing

MDPI

Review

Current Trends in Dissimilar Diffusion Bonding of Titanium Alloys to Stainless Steels, Aluminium and Magnesium

Kavian O. Cooke [1,*] and Anas M. Atieh [2]

[1] Faculty of Engineering and Informatics, University of Bradford, Bradford BD7 1DP, UK
[2] Industrial Engineering Department, School of Applied Technical Sciences, German Jordanian University, Amman 11180, Jordan; anas.atieh@gju.edu.jo
* Correspondence: k.cooke1@bradford.ac.uk

Received: 28 March 2020; Accepted: 26 April 2020; Published: 28 April 2020

Abstract: This article provides a comprehensive review of the advancements made in the diffusion bonding of titanium and its alloys to other advanced materials such as aluminium, stainless steel, and magnesium. This combination of advanced alloys has received considerable attention in different industries, including aerospace, petrochemical, and nuclear applications due to high specific strength, lightweight, corrosion resistance, and moderate to high mechanical properties. The mechanisms of bond formation are discussed based on the type of microstructures formed and the mechanical properties achieved. The scientific literature identifies various methods/processes for controlling the volume of intermetallic compounds formed within the joint regions, as well as ways of maximising the strength of the weld/joints. This paper discusses the relationship between weld/bond properties and bonding parameters such as time, temperature, surface roughness, pressures, interlayer composition, and thickness. The scientific literature also shows that the bonding mechanisms and microstructural evolution of the bond zone can be significantly affected by suitable optimization of the bonding parameters. Additionally, this is a method of maximising bond strength.

Keywords: diffusion bonding; titanium alloys; dissimilar joining; stainless steels; aluminium alloys; magnesium alloys

1. Introduction

In its pure state, titanium exists as a hexagonal close-packed (HCP) structure (α – phase) at room temperature and undergoes an allotropic transformation to body-centred cubic (BCC) (β-phase) when heated to 885 °C [1]. To improve the stability of the α and β phases, titanium is alloyed with elements such a V, Fe, Cu, and Ni. Titanium and its alloys possess a variety of excellent physical, chemical, and mechanical characteristics, which include high strength-to-weight ratio, creep resistance, and corrosion resistance. The benefit that can be derived from these properties ensures that titanium alloys find application extensively in biomedical, chemical, aerospace, and automotive industries because of its superior mechanical and chemical properties when compared to other alloys of similar density. Because of these properties, titanium alloys are often used in the construction of high-performance components such as aero-engines and aircraft manufacturing [2–4].

Although titanium alloys present many unique features for the manufacture of high-performance parts [5–7], the differences between its chemical and thermo-mechanical properties and the unavailability of suitable technology for creating dissimilar joints have restricted its application to the development of single-component systems. However, as the world responds to climate change and the demand for high-strength lightweight systems increases, more research is required to find solutions for dissimilar

joining of advanced alloys and composites for application primarily in automotive and aerospace industries [8–12].

Over the last two decades, several researchers have focused extensively on the development of suitable technologies that are capable of joining dissimilar advanced alloys to form hybrid structures. Researchers are still tackling limitations such as the formation of intermetallic compounds at the interface, galvanic corrosion, slow welding process, and high production cost of the technology [13–17]. This article provides a comprehensive review of the advances made in the diffusion bonding of Ti and its alloys to other advanced structural materials such as aluminium, stainless steel, and magnesium. The paper includes a detailed discussion on the methods of controlling the formation of intermetallic compounds within the joint regions and maximizing weld/bond strength.

1.1. Dissimilar Joining of Titanium Alloys

The development of joining methods for dissimilar alloys will increase their potential applications in the aerospace and automotive industries. However, the joining of these very different alloys which have significant differences in physical and mechanical characteristics presents a great challenge. The differences in the melting point and composition of the alloys dissimilar joining by fusion welding techniques extremely difficult. The heat generated in fusion processes to melting the materials often leads to the formation of various undesirable compounds within the joint zone. During fusion welding, the thermal gradient from a molten weld pool and the parent metal can significantly affect the joint microstructure and phase structure.

The scientific literature contains several fusion welding techniques for dissimilar joining of Ti and other advanced alloys. These techniques include laser welding (LW) [18], resistance spot welding (RSW) [19], friction stir welding (FSW) [20], and friction stir spot welding (FSSW) [21]. Among the available techniques, diffusion bonding [22] has the potential of joining Ti alloys to materials such as aluminium [23], stainless steel [24,25], and magnesium [16,26]. The primary disadvantage of these methods of welding is that the high temperature used in the welding process often leads to the formation of various undesirable intermetallic compounds at the interface [18,27–29]. The presence of thick intermetallic phases at the interface can significantly decrease the bond strength [30,31]. Figure 1 shows a spider diagram that compares the weld/bond efficiency and relative hardness as a function of the joining techniques. The results show that electron beam welding, on average, produces joint strength of approximately 81% that of the base metal. While laser welding and friction stir welding provide the second-highest bond strength, however, the cost of the equipment used in the welding processes is prohibitively expensive in comparison. The weld/bond strength and interface hardness evaluated as a function of the joining techniques were normalized and transformed into percentile representing joint efficiency to make a reasonable comparison between different processes and different alloy combinations.

Table 1 presents a summary of recent research work on dissimilar joining of Ti alloy to stainless steel, aluminium, and magnesium alloys utilizing different joining/welding processes. The table also compares the various alloy couples based on interlayer composition and highlights the associated welding parameter settings for maximising strength (MPa) and hardness (HV) for diffusion couples. The data presented confirm the findings from the spider diagram. Welding processes such as electron beam welding (EBW), LW, and FSW have demonstrated the potential for joining titanium to magnesium, aluminium, and stainless steel. However, numerous limitations restrict the widespread application of these technologies. As demonstrated in Table 1, diffusion bonding is a candidate for joining titanium to other advanced alloys.

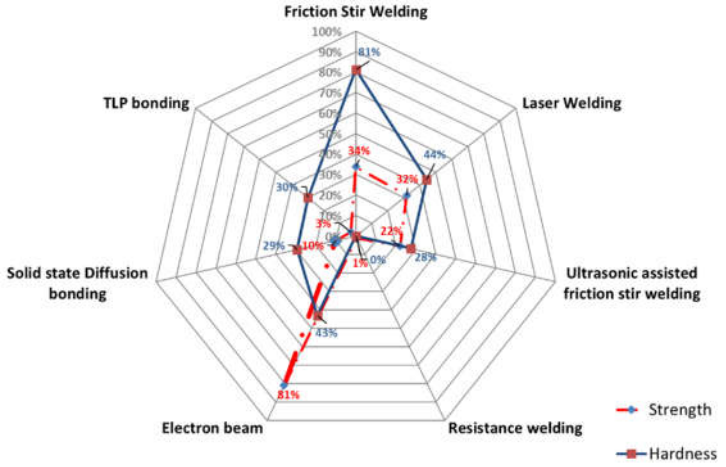

Figure 1. Spider diagram showing the relative joint strength and hardness for dissimilar joints produced by the different welding processes.

Table 1. Recent studies on dissimilar joining of Ti alloy utilizing different processes.

No.	Welding /Joining Process	Parent Materials	Interlayers Materials	Strength (MPa)	Interface Hardness (HV)	Remarks	Ref.
1	FSW	Ti-6Al-4V to 30CrMnSiNi2A	None	490–640	500–800	Increased rotational speed resulted in less thickness of affected interlayer and strength higher than base metal alloy of medium carbon steel.	[32]
2		Pure Ti to Pure Mg	Al foil	150	Not available	As Al foil thickness increased, the welding defects increased due to reduced materials flow.	[33]
3	LW	Ti-Al-V/Al-Cu-Li & Ti-Al-V/Al-Mg-Li	None	250 100	350–450 350–430	Alloying elements affected the joint properties, i.e., Cu vs. Mg such that it increased by 2.5×. Also, the laser beam offset towards Ti alloy.	[34]
4		Al-Cu-Li and Ti-Al-V	None	103–272	Not available	Mechanical characteristics of the intermetallic layer substantially depended on the composition of the alloying elements of the aluminium alloy.	[35]
5		TC4 Ti alloy to 304 austenitic stainless steel	38Zn-61Cu alloy filler	128	100–420	The laser beam at the Ti alloy side and produced a variety of intermetallic compounds at the bond interface.	[36]

Table 1. *Cont.*

No.	Welding /Joining Process	Parent Materials	Interlayers Materials	Strength (MPa)	Interface Hardness (HV)	Remarks	Ref.
6		Ti–22Al–25Nb to TA15	None	943–1011	260–350	O phase was formed in the fusion zone while applying dual-beam laser due to decrease of cooling rate.	[37]
7		TC4 Titanium (Ti) alloy and SUS301 L	None	350	350–450	At the peak temp of 1116 °C, the liquid phase formed and existed only in the narrow region of interface with eutectic phase formation and β-Ti solid-solution.	[38]
8		TC4/TA15	None	50–700	300–420	Coarse β columnar crystals that contain acicular α′ martensitic phase inside fusion zone.	[39]
9	Ultrasonic assisted FSW	Ti-6Al-4V to 6061-T6 aluminium	None	236	60–380	Diffusion like bonding without the intermetallic compounds observed at the joint interface.	[40]
10	RW	Ti-6Al-4V to EW140 glass fabric with PEI	Carbon nanotube lamina	17.3	Not available	Successful joining of Ti alloy to GF/PEI laminate. Welding time severely affected the joining process.	[41]
11	EBW	Ti55 to TA15	None	650–1050	310–380	Formation of martensite α′ and acicular α within the fusion zone.	[42]
12	DB	Ti–6Al–4V to Mg–AZ31	Ni foil	5–45	50–420	Bonding mechanism involves Ni–Mg eutectic formation at the Mg-alloy interface with solid-state diffusion and bond formation at the Ti-alloy interface.	[16]
13		Titanium Alloys and Stainless Steels	Not Available	194	Not Available	Influence of Cu, Ni (or nickel alloy), and Ag interlayers on the microstructures and mechanical properties of the joints.	[25]

Table 1. *Cont.*

No.	Welding /Joining Process	Parent Materials	Interlayers Materials	Strength (MPa)	Interface Hardness (HV)	Remarks	Ref.
14	TLP bonding	Ti–6Al–4V to Mg–AZ31	Ni & Cu nanoparticles	19–69	50–400	Use of Cu nanoparticles as a dispersion produced the maximum joint shear strength of 69 MPa.	[43]
15		Ti–6Al–4V to Mg–AZ31	Ni & Cu foils	12–55	50–400	Formation of phase (Mg), (CuMg2), (Mg2Ni) and Mg_3AlNi_2.	[44]
16		Ti–6Al–4V to Mg–AZ31	Ni electro-deposited coats	26–61	50–350	Increasing the bonding temperature from 500 to 540 ∘C resulted in a change in the bonding mechanism from solid-state to eutectic liquid formation.	[15]
17		Ti–6Al–4V to Al7075	Cu coatings and Sn–3.6Ag–1Cu interlayers	15–42	120–500	Results showed that the Sn–3.6Ag–1Cu interlayer resulted in good joints with a thin Cu interlayer.	[45]

1.2. Diffusion Bonding Process

Diffusion bonding occurs as either solid-state or liquid phase bonding processes. The solid-state variant involves heating of the faying surfaces to a suitable elevated temperature, typically between 60% and 80% of the melting point temperature of the lowest melting point base metal or interlayer. The process contains several steps. The first step involves contact in which surface asperities are deformed as the surfaces to be joined under the effects of heat and static pressure. The second stage is heating, followed by holding the samples at the bonding temperature to facilitate the formation of the joint. During the heating and holding stage of the bonding process, inter-diffusion takes place between the base metals and or base metal and interlayer.

Parameters of importance in solid-state bonding are bonding time, contact pressure, bonding temperature, surface roughness, and interlayer composition [46]. The effect of surface treatment on bond strength varies with the quality of the surface treatments, which can range from an electro-polished finish to turning in a lathe or wire brushing. Figure 2 shows a schematic of the bond set up with a representative heating cycle and process parameters. The results indicate that as the surface roughness increases, the bond strength decreases, which implies that during solid-state bonding, surface roughness is of considerable significance. Higher pressures are typically required to achieve plastic deformation and oxide break-up at the interface and creating an intimate contact between the materials couples.

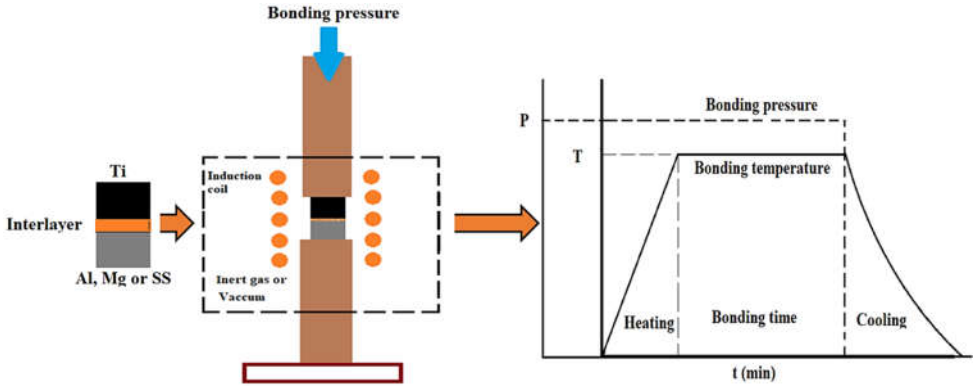

Figure 2. Schematic of the diffusion bonding process and the process parameters (Al—aluminium, Mg—magnesium, and SS—stainless steel).

The second variant of the diffusion bonding is known as transient liquid phase (TLP) bonding. During TLP bonding, a liquid form at the interface wets and spreads between the surfaces by capillary action. Bonding parameters such as temperature, time, interlayer composition, and thickness have a considerable impact on the quality of the weld/bond. However, unlike solid-state diffusion bonding, high pressures are not required to achieve contact between the surfaces. The type of interlayer selected determines the temperature at which liquid forms at the interface. In some cases, interdiffusion between the interlayer and the base metal leads to the formation of eutectic composition, which melts at the bonding temperature. Alternatively, an interlayer having a eutectic or peritectic composition would melt at the bonding temperature [47,48]. TLP bonding contains four stages: heating melting and widening, isothermal solidifications, and homogenization for the bond region. The driving force for the TLP process is the diffusion coefficient, which varies from liquid-phase diffusion during stage 1, to solid-state diffusion during stage two of the bonding process [49].

When the interlayer melts, the liquid wets the base metal surface and is then drawn into the joint by capillary action. The driving force of the bonding process is diffusion, as described by Fick's first and second laws shown Equations (1) and (2). The first law shown in Equation (1) describes diffusion under steady-state conditions while Fick's second law defines a dynamic process in which the composition of the joint zone changes with time

$$J = -D\frac{\partial C}{\partial x} \tag{1}$$

Fick's second law describes a non-steady state diffusion in which the concentration gradient changes with time

$$\frac{\partial C}{\partial t} = D\frac{\partial^2 C}{\partial x^2} \tag{2}$$

a general solution for Equation (2) using separation of variables is [50]

$$C(x,\ t) = \frac{1}{2\sqrt{D\pi t}}\int_{-\infty}^{+\infty} f(\xi)e^{\left(\frac{\xi-x)}{4Dt}\right.}d\xi \tag{3}$$

where the error function solution for this equation is

$$C(x,\ t) = \frac{C_0}{2}\left[erf\left(\frac{x-x_1}{\sqrt{4Dt}}\right) - erf\left(\frac{x-x_2}{\sqrt{4Dt}}\right)\right] \tag{4}$$

2. Effect of Bonding Parameters

2.1. Bonding Time and Temperature

Interdiffusion between Ti/SS, Ti/Al, or Ti/Mg often leads to the formation of various reaction layers at the interface. The parabolic law shown in Equation (5) estimates the width of the reaction layer. The rate of formation of the reaction layer can be determined using Equation (6), which also demonstrates the impact of temperature and activation energy on the growth rate of the reaction layer.

$$x = \sqrt{Kt} \tag{5}$$

where

$$K = K_o e^{\frac{-Q}{RT}} \tag{6}$$

where x is the thickness of the reaction layer, K is the rate factor, t is the diffusion time, and n is the time exponent. The use of the parabolic law suggests that volume diffusion controls the growth kinetics of the intermetallic layer; therefore, diffusion time is $t^{1/n}$ where n =2. Figures 3 and 4 shows the relationships between the thickness of the reaction, bonding time, and temperature for Ti/stainless

steel and Ti/Mg couples. The Arrhenius type rate equation presented in Equation (6) confirms that the bonding temperature is directly proportional to the growth rate of the reaction layer.

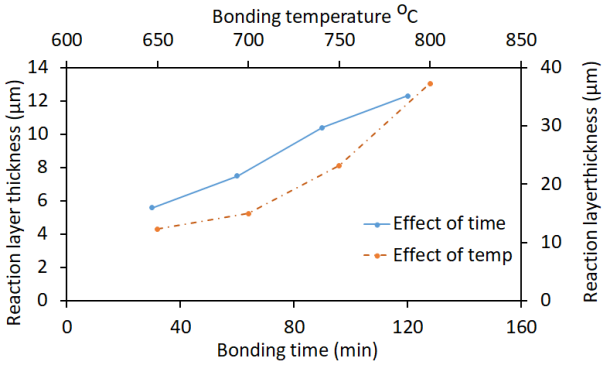

Figure 3. Relationship between the width of the reaction layer bonding time for Ti-6Al-4V and 316 stainless steel [59].

Diffusion bonding between titanium alloys and stainless steels typically occurs at higher temperatures than would be used for Ti/Al and Ti/Mg couples, since Al and Mg had a much lower melting point temperatures than stainless steels. Diffusion bonding in titanium to stainless steel typically occurs within the temperature range of 650–950 °C. In a study conducted by Velmurugan et al. [51], the authors studied low-temperature diffusion bonding of Ti-6Al-4V and Duplex stainless steel within the temperature range of 650–800 °C and external pressure of 10 MPa. The results of the study showed that both the thickness of the reaction layer and shear strength of the joint increased with increasing bonding temperature from 140 MPa at 650 °C to 192 MPa at 750 °C, this may represent an increase of 27% in bond strength. Further increase in temperature resulted in the bond strength, decreasing to 174 MPa, hence resulted in a 9% decrease of the achieved bond strength. The formation of a larger volume of intermetallic compounds at higher temperatures caused a reduction in bond strength. The literature shows that the thickness intermetallic layer formed at the interface increased with increasing temperature above a specific limit (750 °C). In another study [52], it found that when Ti-6Al-4V is diffusion bonded to ferritic stainless, mutual distribution of Fe and Ti controlled the interface microstructure. However, in this study, the maximum joint strength of 187 MPa at 980 °C. The differences in the bonded strength may be attributed to changes in the composition of intermetallic compounds formed at higher temperatures [53].

Additionally, the author showed that the thickness of the FeTi intermetallic phase layer decreased by increasing the process temperature; however, the width of the Fe_2Ti layer in the interface region increased. Consequently, samples bonded below 880 °C experienced failure through the FeTi layer. The literature showed that a bonding time of two hours ensured optimum bond strength between titanium alloys and stainless steels.

Li et al. showed that for the diffusion bonding of Ti-17 alloy at a bonding temperature of 860 °C and bonding pressure of 3 MPa not only the voids percentiles but also their average size has a reverse relation with bonding time. Furthermore, as the bonding time increased, the shape of voids transformed from irregular shape to ellipse then to small circular shape, this reduction in voids amount and size increased shear strength to 887.4 MPa at 60 min bonding time [54].

The conditions used for bonding titanium to aluminium and magnesium alloys are significantly different from those used for diffusion bonding Ti/stainless steel couples. The scientific literature shows that the melting point of the aluminium or magnesium alloy constrains the bonding temperature during the diffusion bonding of Ti/Al or Ti/Mg couples. Given the differences in thermo-mechanical properties between titanium, aluminium, and magnesium, require substantially shorter bonding time, and lower bonding temperatures are necessary. Diffusion bonding of Ti/Al couples typically occurs between 500 and 600 °C [55,56]. Rajakumar et al. [57] used a desirability function with a response

surface modelling (RSM) to optimise the parameters for diffusion bonding titanium to aluminium alloys. The results of the study showed that at a bonding temperature of 510 °C, a bonding time of 37 min, and pressure of 17 MPa, the joint strength can be maximised. Transient liquid phase diffusion bonding of Ti/Al and Ti/Mg couples utilises a low melting interlayer between the base metal alloys.

The interlayer may melt at the bonding temperature or react with the base metals to form a eutectic liquid at the bonding temperature. The transient liquid wets the surface and spreads by capillary action between the faying surfaces. The eutectic reaction removes the surface oxides and ensures metal-to-metal contact [58]. The capillary action provides the principal driving force for liquid-phase joining. The free energy of the metal surfaces aids the capillary action depending on the contacting liquid or gaseous phase. The primary parameter is the contact angle "θ" which provides a measure of the wettability of the surface by the liquid filler metal. The contact angle is defined as the angle between the solid–liquid and liquid–gas surface tensions and can be determined using Equation (7).

$$Cos\ \theta\ =\ \frac{\gamma_{SV}\ -\ \gamma_{SL}}{\gamma_{LV}} \tag{7}$$

where: γ_{SV} is the surface free energy at the solid–vapour interface γ_{SL} is the surface free energy at the solid–liquid interface and γ_{LV} is the surface free energy at the liquid–vapour interface.

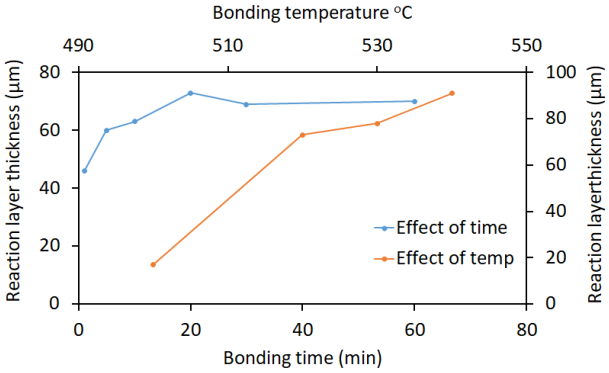

Figure 4. Relationship between the width of the reaction layer and bonding time for Ti-6Al-4V and magnesium Az31 [17].

The total bonding time includes the duration of the heating stage and the period of holding at the bonding temperature. During the heating stage, the entire assembly heated in a vacuum or inert atmosphere (argon or helium) to the bonding temperature. The mass transferred by interdiffusion taking place within the heating stage is dependent on the rate of heating and the bonding temperature. A longer heating rate will result in the diffusion of more of the interlayer into the base metal. However, if the heating stage is too long because the heating rate is too slow, the maximum composition of solute in the interlayer may dip below the solidus composition at the bonding temperature, and no liquid will form upon further heating. While this problem does not affect solid-state diffusion bonding, it will severely impact TLP bonding using very thin interlayers.

Li et al. [60] used Fick's second law to develop a model for the prediction of bonding time and its probability distribution during diffusion based on the stochastic characteristics of the surface finish of the bonded area. Equation (8) provides a probabilistic model for calculating the bonding time.

$$t = \int_{f_o}^{f} \frac{-\sigma_e / \dot{\varepsilon}}{\left(3p\sqrt{f} - \frac{2\gamma\sqrt{f}}{r_o} + \frac{2\gamma}{r_o}\right) + \frac{2r_o^2 p}{ln\left(\frac{1}{f}\right) - \frac{1-f}{2}\frac{\Omega}{KT}}\left[\frac{1+\frac{h}{d}}{h} D_{gb\delta} + 2\Omega D_v\right]} df \tag{8}$$

where σ_e, $\dot{\varepsilon}$ is Levy–Mises effective stress and effective plastic strain rate, respectively. P is the external pressure; T the temperature (K); γ the surface energy; A, Q, and n are the Dorn constant in power-law

creep equation, activation energy and creep, exponent, respectively. The application of Fick's second law shows that the rate of change in f, which is caused by grain boundary diffusion and volume diffusion. Where Ω is the atomic volume, D_{gb}, D_v the grain boundary diffusivity and volume diffusivity, δ, d, and h are the grain boundary width, grain size and void height, respectively.

2.2. Pressure and Surface Roughness

The roughness of the faying surfaces is critical in diffusion bonding since the quality of the initial surface contact has a significant impact on the real contacting area and the mass solute atoms diffusing during the heating stage of the bonding process. As an integral part of the bonding process, the surface finish determines the first surface contact area and the size of the voids at the interface. The quality of the surfaces is dependent on the technique for preparation; a smooth surface finish is better to ensure excellent initial contact for transient liquid phase bonding. Zuruzi et al. [61] found that rougher surfaces yielded superior ultimate tensile strength; however, the number of incomplete bonds increased as the surface roughness increased. In a similar study applied to diffusion bonding copper, the results showed that the tensile strength of the joint decreased with increasing surface roughness, as shown in Figure 5. Additionally, the data showed that the joint efficiency increased with reduced surface roughness. This behaviour was attributed to incomplete contact and plastic deformation at the interface for rough surfaces during the initial stages of bonding. The scientific literature shows that during solid-state diffusion bonding of Ti to base metals such as aluminium, stainless steel, and magnesium [62]. The impact of increasing bonding pressure is increased plastic deformation of the asperities at the interface, which also increases the real area of contact. The microstructure formed at the interface during solid-state diffusion bonding of Ti/SS, Ti/Al, and Ti/Al couples improves with increasing bonding pressure. However, given the similarities of the mechanical properties of Ti and stainless steels, higher pressures are typically required for joint Ti/SS couples than the bonding pressure needed for Ti/Al and Ti/Mg couples.

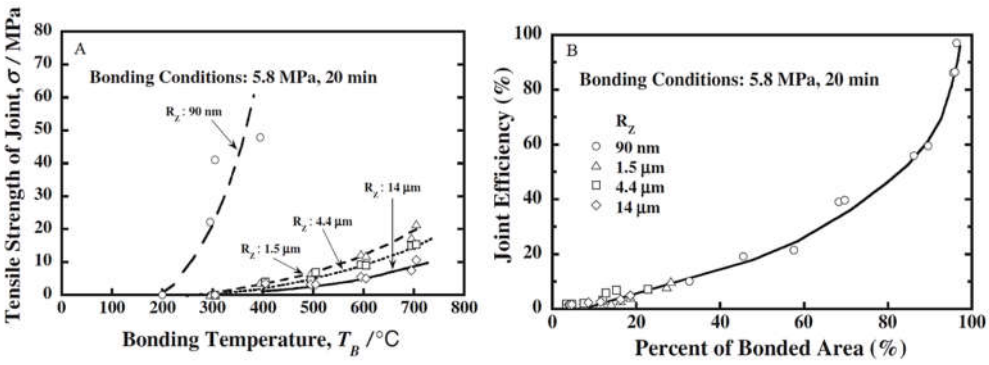

Figure 5. (**A**) Relationship between the tensile strength of joints and bonding temperature for various surfaces prepared by lathe machining method. (**B**) Relationship between joint efficiency and percentage of the bonded area for multiple surfaces [63].

Liquid phase diffusion bonding, on the other hand, has been shown to use much lower external pressure than solid-state diffusion bonding. Nominal weight is typically used in TLP bonding since high pressure would squeeze the liquid from within joint [15]. Surface roughness also influences the interlayer thickness since the maximum liquid width must be larger than the average surface roughness to ensure that the liquid phase sufficiently wets the base metal at both interfaces. Also, given that only minimal pressure is required in TLP bonding to provide metal-to-metal contact, the removal of surface contaminants and thick oxides before bonding is crucial to guaranteeing intimate contact at the interface, under low-pressure bonding. Samavatian et al. [64] studied the impact of pressure on the diffusion bonding of Ti-6Al-4V using Cu interlayer. The results showed that although the width of the bond zone decreased with increasing bonding pressure. Conversely, while the width of the bond

region decreased, the bond strength increased to a maximum value of 571 MPa at a bonding pressure of 4 MPa. The reduction in the width of the bond region was attributed to liquid squeeze out during the bonding process.

2.3. Interlayer Composition and Thickness

The addition of an intermediate material between the two base metals improves the quality of the bond. In addition to the composition and thickness of interlayer, the different interlayer format may affect the joint formation, for instance, foils, coats, and nanoparticles have been used as an interlayer to establish the bond or to accelerate the bond formation.

Various interlayers have shown varying degrees of success in joining titanium to other advanced alloys such as titanium alloys to stainless steels, aluminium alloys, and magnesium alloys. Figure 6 shows a Ti/Steel joint bonded at 700 °C. In instances where titanium is diffusion bonded to stainless steels, intermetallic compounds such as FeTi and Fe_2Ti form at the interface [65]. The presence of thick intermetallic layers at the interface severely limits bond strength and reduces the mechanical capabilities of the joint [31]. The Gibbs energy of formation suggests that the compound FeTi typically forms first with an activation energy of 124.9 kJ/mol [66]. The presence of the FeTi intermetallic within the joint zone has a detrimental effect on joints made below 850 °C. For samples bonded at 900 °C intermetallic compounds such as Ti_2Fe and TiFe at the interface [31]. The Fe_2Ti (Cr, Ni) intermetallic typically forms at a higher temperature with an activation energy of 125.8 kJ/mol [66] and its impact on the mechanical properties of the joint has been shown to less damaging since the compound generally forms as discontinuous phases within the joint zone. Compounds such as Cr_2Ti(Fe) may also develop in diffusion bonded couples of stainless steel (AISI 316) and commercially pure titanium at 950 °C [66].

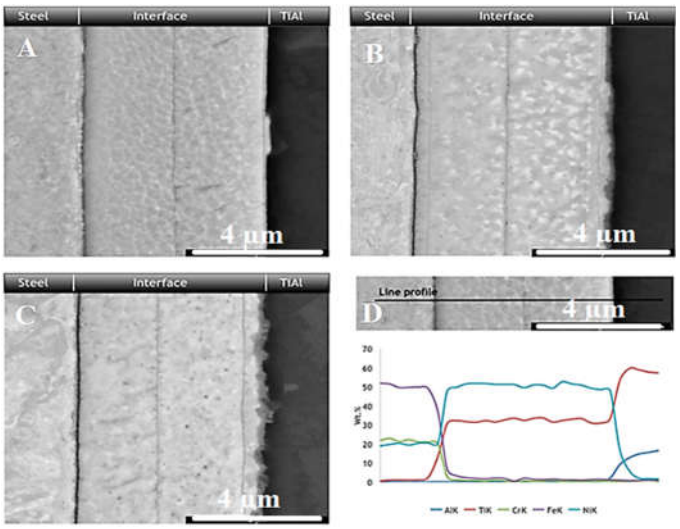

Figure 6. Scanning electron microscope (SEM) micrographs of the TiAl/steel joints produced at; (**A**) 700 °C under a pressure of 50 MPa using Ni/Ti multilayers with 30 nm of bilayer thickness; (**B**) 800 °C under a pressure of 10 MPa using Ni/Ti multilayers with 30 nm of bilayer thickness; (**C**) 800 °C under a pressure of 10 MPa using Ni/Ti multilayers with 60 nm of bilayer thickness and (**D**) Energy dispersive spectroscopy (EDS) profile across the interface presented in (**A**) [67].

The addition of an intermediate material between the faying surfaces modifies the composition and structure of the intermetallic layers. Interlayers such as Ni [65], Cu/Nb multilayer [59], Ag [53], Cu/Al_2O_3 [68], Al [69], Cu [70], and Sn [71], have demonstrated the ability to modify the type of reaction layers that form at the interface. The addition of monolithic interlayers prevents the formation of intermetallic compounds between Ti and stainless steel (see Figure 6). New intermetallic compounds form between the interlayer materials and the base metals. The use of aluminium interlayer prevents

the formation of intermetallic compounds between Ti and Fe. However, intermetallics of $FeAl_6$, Fe_3Al, and $FeAl_2$ form at the Al/SS interface. The presence of intermetallic compounds at the interface severely decreases the strength of the bond formed. The use of copper as the interlayer during diffusion bonding of Ti to stainless steels results in the formation of a eutectic liquid at the bond interface which has been shown to decrease the volume of intermetallic compounds forming at the interface but does not prevent its development [24,70,72]. Recent studies have shown that embedding Al_2O_3 nanoparticles in the Cu interlayer reduces the width of the intermetallic layer that forms at the interface and decreases the grain sizes within the bond region. Figure 7 shows a comparison of joint bonded with Cu-foil and Cu coating containing Al_2O_3 nanoparticles. The composition of each phase is presented in Table 2 [68].

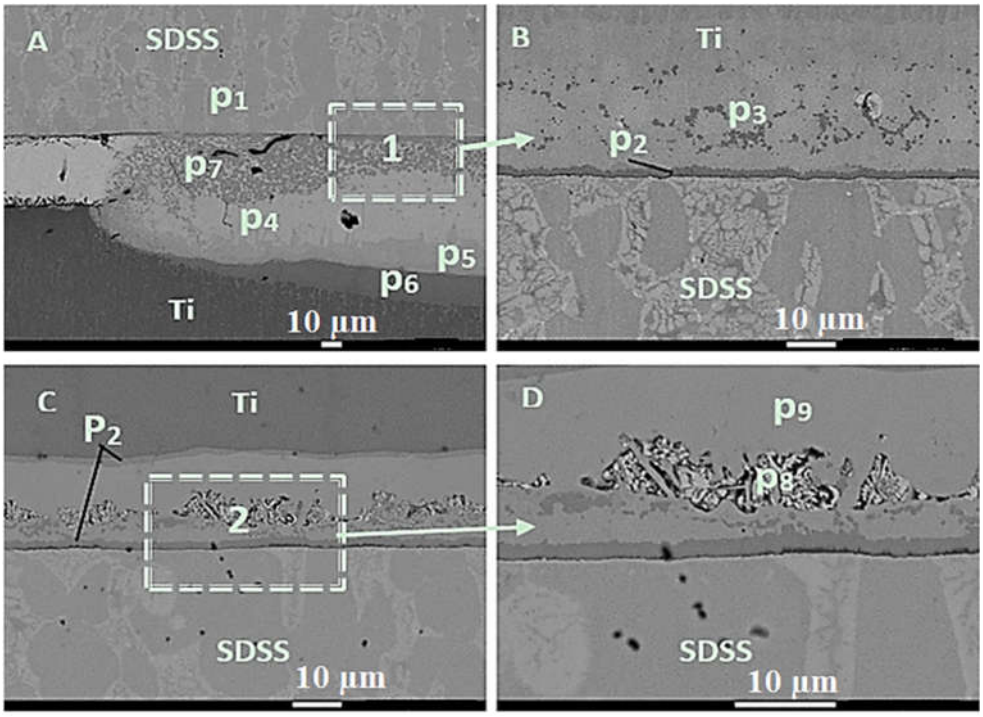

Figure 7. (**A**) Diffusion bonding of Ti-6Al-4V and super-duplex stainless steel (SDSS) using Cu/Al_2O_3 interlayer for 30 min at a bonding temperature of 850 °C; (**B**) Detail micrograph of the region-1; (**C**) Ti/SDSS couple joined using 25 µm Cu-foil interlayer for 30 min at a bonding temperature of 850 °C; (**D**) Detail of region-2 [68].

Table 2. Composition of the bond interface measure with EDS (wt %) [68]

Phase	Al	Ti	V	Fe	Cu	C	Cr	Ni	Possible Phase
p_1	-	0.22	-	61.57	0.68	3.51	24.45	5.73	
p_2	1.86	28.64	1.03	0.54	67.34	-	-	0.59	$TiCu_2$
P_3	2.43	33.78	1.24	1.26	58.45	2.34	-	-	$TiCu_2$
P_4	0.32	41.31	0.73	-	55.54	2.1	-	-	TiCu
P_5	1.36	41.55	1.40	1.13	51.32	2.89			TiCu
P_6	5.53	79.00	4.83	0.45	10.18	-	-	-	Ti_2Cu
P_7	7.49	47.08		1.95	40.47	1.47	1.08	0.46	$TiCu\text{-}Al_2O_3$
P_8	1.35	41.55	1.40	1.13	51.32	2.89	0.36	-	$Ti_x\ Cu_x\text{-}Fe_x$
P_9	2.19	54.19	1.91	0.81	37.77	2.58	0.29	0.26	Ti_2Cu

Joining titanium alloys to heat treatable aluminium and magnesium alloys experience similar challenges to those encountered when diffusion bonding titanium to stainless steels [57]. The oxide film present on the surfaces of both the titanium and the aluminium alloys severely hampers bond formation. The scientific literature shows that diffusion bonding of Ti/Al couples often leads to the

precipitation of intermetallic compounds such as TiAl and Ti_3Al [56]. Additionally, the presence of an oxide layer on the surface of the Ti and Al surfaces reduces the chances of metal-to-metal contact during the bonding process and decreases the efficiency of the joint. The use of intermediate materials at the interfaces ensures that the faying surfaces are wetted and change the types, shape, and sizes of the intermetallic compounds formed at the interface. The use of Cu as an intermediate material at the interface between Ti-6Al-4V and Al 7075 leads to the formation of compounds such as $\theta(Al_2Cu)$, $T(Al_2Mg_3Zn_3)$ and Al13Fe within the alloy. Additionally, the diffusion of Cu into the titanium alloy results in the formation of Cu_3Ti_2 [73].

Interdiffusion at the Ti/Al or Ti/Mg interfaces causes the formation of intermetallic compounds. Figure 8 shows the microstructure produces when Mg-AZ31 is bonded directly to Ti-6Al-4V. Solid-state diffusion bonding of Ti/Mg couples has been demonstrated in previous studies however the results of these studies show that within these diffusion couples Al reacts with Ti and Mg leading to the formation of the $TiAl_3$ and $Ti_2Mg_3Al_{18}$ intermetallic compounds at the Ti interface. Additionally, $Mg_{17}Al_{12}$ intermetallic compounds appear to have formed at the Mg grain boundaries. The joint formation occurs because of a metallurgical bonding leading to the precipitation of $TiAl_3$ and $Ti_2Mg_3Al_{18}$ [23].

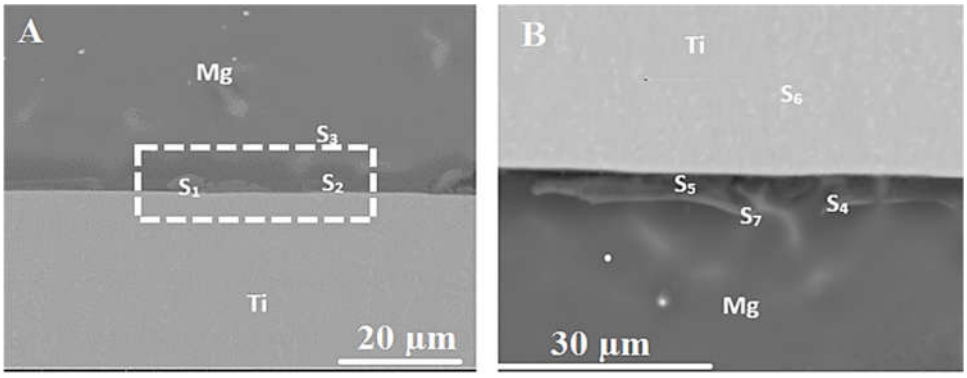

Figure 8. (**A**) Solid-state diffusion bonding of Ti and Mg for 60 min; (**B**) magnified region of the bond-line showing the reaction layer at the bond interface [23].

On the other hand, transient liquid phase diffusion bonding of Ti/Mg couples shows a varying degree of success with various interlayers. Intermediary materials such as Cu [74], Ni [15], Cu/Al_2O_3, Ag, Zn, and Sn. Figure 9 shows a Ti-6Al-4V/Mg (AZ31) joint bonded with Ni/Al_2O_3 used as the interlayer the nanoparticles successful in modifying the size and shape of the intermetallic structures present at the interface.

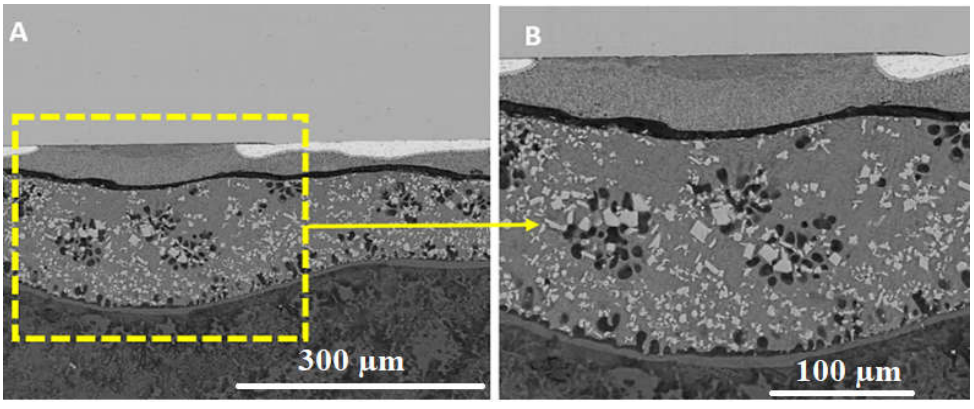

Figure 9. (A) Ti and Mg joint bonded using Ni/Al_2O_3 interlayer for 60 min at 500 °C (**B**) Detailed view of the highlighted region.

Considering the Mg to Ti alloy system, Zhang et al. studied the effect of Cu coating thickness on the interfacial reaction in laser welding/brazing of Mg to Ti. In their work, they have electrodeposited the Cu coating on the titanium alloy. Intermetallic compounds such as; Ti_3AL, Ti_2Cu, and $AlCu_2Ti$ formed at the interface. These intermetallic evolved with an increase of Cu coating thickness. The thermodynamic calculations suggest that Cu promotes the mutual diffusion of Ti and Al. However, the Ti-Al reaction is preferred compared to Ti-Cu. The presence of Cu enhanced the joint strength by 55% compared to similar Ti-Mg dissimilar joint without Cu [75].

Ti-6Al-4V alloy coated with Cu-Ni were laser welded/brazed to Mg-AZ31 alloy. It was observed that Al-Ni-Ti, Ti_3Al, and Ti_2Ni were produced at the bond interface when 15.4 µm Ni and 5.5 µm Cu was utilized as an interlayer. A critical interlayer thickness of 10 µm produces a sound joint. Interestingly, when the Cu layer increased significantly (17.1 µm) compared to Ni (4.2 µm), only Ti_3Al phase formed inside the joint interface. This increase in Cu and decrease in Ni resulted in increased then decrease of bond strength, the maximum achieved strength of 2.02 kN at comparable Cu and Ni thickness [76].

The scientific literature shows that the composition of the interlayer has a considerable impact on the microstructure and mechanical properties of the joints formed during diffusion bonding. Table 3 shows a summary of the influence of interlayer composition. The quality of the joint produce when bonding base metal-1 to basemetal-2 using an interlayer is labelled E, G, F, P, or N to represent the soundness of the bond produced as a function of joint efficiency. Where E means excellent for joint with efficiency higher than 80%, G is for Good (efficiency between 61–79%), F is for Fair (efficiency between 50–60%), P- Poor (efficiency below 50%), and N means data is unavailable for the specific combination. The results show that the bond efficiency Ti/Al as a function of interlayers varied from 'Fair' to 'Poor' with Cu, Ga, and Sn-5.3Ag-2Bi producing bonds with the best properties. When bonding Ti/Mg couples Cu/Al_2O_3, Ni, and Cu have demonstrated considerable potential for producing sound bonds. Similarly, diffusion bonding of Ti/SS couples using monolithic interlayer such as Ag, Cu has shown significant promise. Additionally, the literature indicates that alloyed interlayers such as Cu-Nb, V-Cr-Ni, and Ni–17Cr–9Fe are best suited when diffusion bonding Ti to stainless steels.

Table 3. Composition of interlayers used during diffusion bonding Ti/Al, Ti/Mg and Ti/SS couples with the following key: E—excellent, G—Good, F—Fair, P—Poor, N—No data.

Base Metal 1	Interlayer Material	Basemetal-2					Ref.
		Al Alloys	Mg Alloys	Stainless Steels			
				Ferritic	Austenitic	Duplex	
Ti	None	N	P	G	G	F	[23,66,77,78]
Ti	Cu	F	F	F	G	F	[24,73,79–81]
Ti	Ni	N	F	F	F	F	[15,74,82]
Ti	Ag	N	N	E	G	G	[83,84]
Ti	Al	N	N	F	F	N	[67]
Ti	Ga	F	N	N	N	N	[85]
Ti	Cu-Nb	N	N	G	G	N	[59]
Ti	Nb/Cu/Ni	N	N	F	F	F	[86]
Ti	Cu-Zn	P	N	N	N	N	[87]
Ti	Cu-Ni	N	P	N	N	N	[43]
Ti	Ni/Al_2O_3	N	N	N	N	G	[68]

Table 3. *Cont.*

Base Metal 1	Interlayer Material	Basemetal-2					Ref.
		Al Alloys	Mg Alloys	Stainless Steels			
				Ferritic	Austenitic	Duplex	
Ti	Cu/Al_2O_3	N	G	N	N	N	This work
Ti	V-Cr-Ni	N	N	E	E	N	[88]
Ti	Ni–Cr–B	N	N	N	N	F	[89]
Ti	Sn-3.6Ag -1Cu	P	N	N	N	N	[45]
Ti	Sn-10Zn-3.5Bi	P	N	N	N	N	[55]
Ti	Sn-4Ag-3.5Bi	P	N	N	N	N	[90]
Ti	Sn-5.3Ag-2Bi	F	N	N	N	N	[91]
Ti	Al-Si-Cu-Ge	F	N	N	N	N	[92]
Ti	Ni–17Cr–9Fe	N	N	N	N	G	[77]

3. Mechanical Performance of Joints

A critical consideration driving dissimilar joining is the desire to maximise the strength of the resulting weld/joint while minimising unwanted reactions that lead to the formation of intermetallic compounds within the joint zone. The aim of dissimilar welding and joining of Ti alloy is to maintain the mechanical properties of the Ti base metal alloy. The mechanical properties depend on the amount of heat input into the material during the joining/welding process and the parameters of the welding/joining process. In general, the dissimilar joints assessed by bond strength, high fatigue resistance, asymmetric hardness profiles, and moderate to high shear strength. The mechanical properties of the joint depend on the mechanism of joint formation, and specifically the formation of intermetallic compounds and phases within the joint region. The presence of intermetallic compounds within the bond area often play a significant role in the integrity of the joint.

Alhazaa [73] demonstrated that the Ti-6Al-4V and be successfully bonded to Al7075 using an appropriate intermediate material. As shown in Table 3, Ti/Al couples bonded interlayers Cu, Ga, and Sn-5.3Ag-2Bi producing bonds with the best properties. However, in these cases, the formation of intermetallic compounds at the bond interface still has the potential of compromising the bond strength. Similar findings were reported by Atieh and Khan [15], who showed that the use of Ni and Cu interlayers demonstrate the considerable potential for producing sound bonds.

Balasubramanian investigated diffusion bonding of titanium alloy and 304 stainless steel using Ag as the interlayer and characterised the impact of process parameters on hardness, stiffness, and the width of the reaction layer formed at the interface [5]. The study showed a bond shear strength of 158 MPa at a bonding temperature of 800 °C, which corresponds to a joint efficiency of 77%. The literature suggests that temperature has the most significant effect on the shear strength of the bond, followed by the holding time and pressure [5]. In his other study, Balasubramanian reported that as traditional welding techniques are not suitable to join titanium alloy due to its affinity to nitrogen and oxygen from the atmosphere. When titanium alloys were bonded to 304 stainless steel using fusion welding, brittle intermetallic compounds formed inside the joint region and deteriorated the mechanical strength of the joint. As a result, diffusion bonding is an alternative for joining this dissimilar system. The bonding parameters studied include: bonding temperature from 650 to 825 °C, bonding pressure from 2–5 MPa and bonding time from 30–120 min. The results showed that the maximum shear strength of 158 MPa was achieved with parameter settings of 800 °C, 5 MPa for 90 min [53].

Kundu et al. [72] diffusion bonded commercially pure titanium to 304 stainless steel using 300 µm Cu interlayer. The bonding in the temperature range of 850–950 °C for 1.5 h under 3 MPa uniaxial load

in a vacuum. The authors indicated that though the Cu interlayer was not able to block the diffusion of Fe, Cr, and Ni to the Ti side and Ti to 304-SS side and developed a bond strength of 318 MPa with 8.5% ductility. In another study, Kundu et al. [93] demonstrated successful diffusion bonding of Ti-6Al-4V and micro-duplex stainless steel. The bonding parameters studied include: bonding temperature of 850–1000 °C, bonding time of 45 minutes under vacuum. The high temperature used in the process led to the formation of several intermetallic phases at the interface. These include; σ, λ + FeTi and λ + FeTi + β-Ti phase mixtures for samples bonded at 900 °C or higher. Higher bonding temperature increased the volume of intermetallics compounds formed withing the joint zone. Maximum bond strength was recorded for samples bonded at 900 °C and corresponded to a thin intermetallic layer at the interface.

4. Mechanisms of Bond Formation

Solid-state diffusion bonding of Ti-SS, Ti-Al, and Ti-Mg couples typically occur in several stages. Figure 10 shows a schematic of the solid-state diffusion bonding process. The first stage of the solid-state diffusion bonding process is the initial contact at the faying surfaces under the applied pressure. The applied force causes plastic deformation of the faying surface and increases the area of contact. The quality of the surface finish will determine the height of the asperities present at the surface and controls the real area of contact. Stage two of the bonding process involves heating the assembled samples to the bonding temperature. According to MacDonald and Eager during the heating stage up to the bonding temperature, the effect of diffusion into the interlayer can be neglected until 80% of bonding temperature achieved.

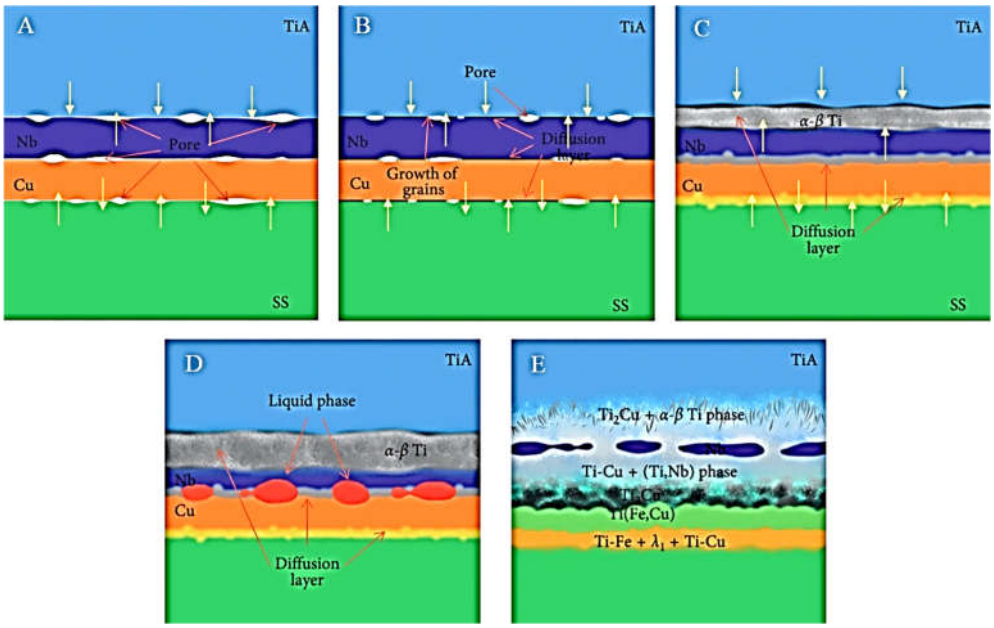

Figure 10. Formation process of titanium alloy and stainless steel diffusion-bonded joint using Cu/Nb multi-interlayer: (**A**) pores exist at the interface; (**B**) diffusion of atoms and growth of grains; (**C**) formation of α-β Ti and diffusion layers; (**D**) liquid phase formed at the interface; (**E**) formation of intermetallic compounds [25].

The application of external pressure and the combination of heating facilitates additional plastic deformation at the interface, which results in void closures that displace surface oxides and increased metal-to-metal contact. Stage three involves holding the assembly at the bonding temperature, which facilitates interdiffusion between the base metals or the base metals and the interlayer. At the bonding temperature, interdiffusion leads to the formation of a reaction layer at the interface. The final stage of the bonding process is the homogenization of the bond region. The driving force for the homogenization stage of the bonding is diffusion, which is also dependent on the bonding temperature.

The mechanism of bond formation during liquid phase bonding includes five distinct stages, as shown in the schematic in Figure 11 [68]. The first stage of the process is heating during which interdiffusion between the interlayer and the base metals causes the composition of the joint region to changes, and this stage is very similar to the first stage seen at the solid-state diffusion. However, the first stage causes an increase of element concentration interdiffusion, which leads to eutectic liquid reaction takes place at the bonding temperature, which affects the following steps. The second stage of the process is dissolution and widening during this stage of the bonding process, the interlayer melts, and the joint zone widens due to the changing composition of sections of the base metal. The effect of pressure and capillary action resulted in the spread of the liquid eutectic along with the bond interface. The thermodynamic evaluation of the reaction follows the specific binary/ternary phase diagram for those combinations: Ti-Al-Mg, Ti-Al-Fe, Ti-Al, Ti-Mg, and Ti-Fe. The increase in bonding time resulted in more spreading of the liquid eutectic and an increase in the contact area between the bonded alloys.

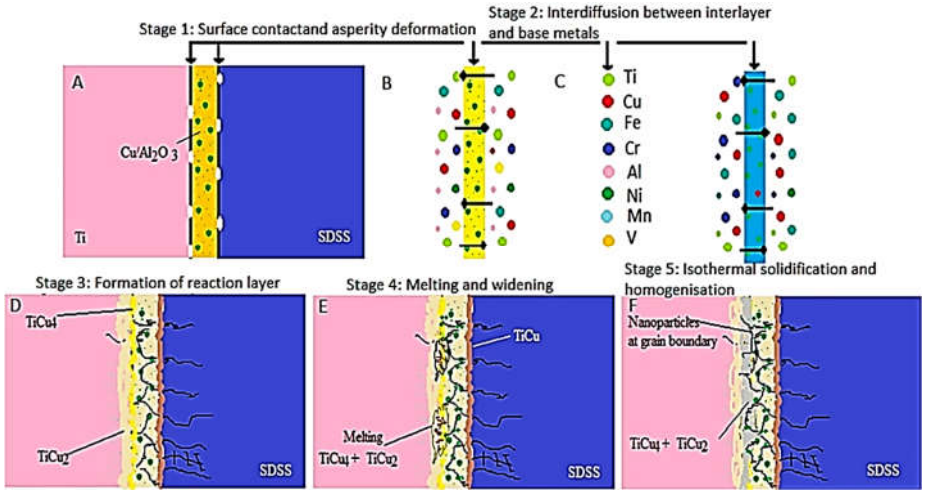

Figure 11. A schematic of the mechanism involved in the bond formation of Ti–6Al–4V and super-duplex stainless steel using a Cu/Al_2O_3 interlayer: (**A**) initial surface contact and asperity deformation; (**B**,**C**) interdiffusion between interlayers and base metals; (**D**) formation of the reaction layers; (**E**) eutectic melting which occurs in samples bonded at 900 °C; (**F**) isothermal solidification and homogenization of the interface [68].

Stage three includes the isothermal solidification of the liquid interface. The joint region solidifies due to continued interdiffusion within the interface which pushed the composition of the area below the solidus line, and the driving force for this stage to occur is the difference between liquidus concentration between the two base metal alloys. The scientific literature showed that diffusion during the isothermal solidification is the most significant factor affecting joint quality. Tuah-Poku et al. [49] demonstrated that the duration of the isothermal solidification stage is proportional to the maximum obtained width and inversely proportional to the diffusion coefficient. The final stage of the bonding process involves the homogenization of the bond region. This stage of the bonding process requires a longer holding time, which allows the eutectic residual to diffuse away from the interface. The exact duration of this stage is unclear and could last anywhere from several minutes to several hours.

5. Key Challenges and Future Direction

Although extensive research work has occurred in dissimilar joining/welding of advanced alloys, Ti/SS, Ti/Al, and Ti/Mg couples there still exist numerous challenges that have not been successfully addressed by existing research. Multiple research groups are investigating the use of diffusion bonding as a method of dissimilar welding. The intermetallic formation at the interface remains a significant issue that still needs further attention. Recent research work has demonstrated that the addition of ceramic nanoparticles to the interlayer has the potential of disrupting the continuous intermetallic

layer while simultaneously producing smaller grains such that it works as reinforcement inside the joint region.

Additionally, the diffusion bonding process is substantially slower all the other available welding processes capable of welding titanium to other alloys. Successful integration of DB into current manufacturing practises, demands an increase in the speed at which the samples can be welded/bonded. A clear example of this is the application of 3D metallic printing to generate nanostructure interlayers for diffusion/TLP bonding. The large surface to volume ratio of the nanomaterials and the high surface energy decreases the duration of the bonding process and reduced bonding temperature. Utilization of different heat sources for better process control is needed; currently, most research work on diffusion bonding and TLP focuses on induction heating.

Transient liquid phase bonding of these advances alloys does reduce the bonding time from hours to approximately 30 min, but further improvements in the speed of the process are still needed. Another limitation of the application of diffusion bonding is the type/configurations of the joints that can be made by the process. The process typically utilizes butt joints or lap joints since large surface areas are required to ensure interdiffusion between the base metals and the interlayer.

As research into diffusion bonding continues, bond efficiency (Ti/Al, Ti/SS, and Ti/Al) will increase as the technology matures. Additional research is also required to develop suitably automated diffusion bonding systems that integrate mechanisms for assessing the quality of the weld/bond. Further studies are also needed to explore the development of smart joints/welds, which can communicate with an externally connected system when the weld/bond has come to the end of its useful life.

The development of standards to support the proliferation of technology in a way that gives manufacturers the confidence. Finally, the provision of education and training for technical staff who will be required to use this technology. These changes would ensure that diffusion bonding is a desirable alternative to conventionally available techniques.

Author Contributions: Research and Writing—original draft, K.O.C. and A.M.A; Writing—review and editing, K.O.C. and A.M.A. All authors have read and agreed to the published version of the manuscript.

Funding: This research received no external funding.

Conflicts of Interest: The authors declare no conflict of interest.

References

1. Peters, M.; Hemptenmacher, J.; Kumpfert, J.; Leyens, C. Structure and Properties of Titanium and Titanium Alloys. In *Titanium and Titanium Alloys*; Wiley: Weinheim, Germany, 2005.
2. van Beek, J.A.; Kodentsov, A.A.; van Loo, F.J.J. Phase equilibria in the CuFeTi system at 1123 K. *J. Alloys Compd.* **1995**, *217*, 97–103. [CrossRef]
3. De Viteri, V.S.; Fuentes, E. Titanium and Titanium Alloys as Biomaterials. In *Tribology - Fundamentals and Advancements*; Intech: London, UK, 2013.
4. Leyens, C.; Peters, M. *Titanium and Titanium Alloys*; Wiley: Weinheim, Germany, 2003.
5. Balasubramanian, M. Characterization of diffusion-bonded titanium alloy and 304 stainless steel with Ag as an interlayer. *Int. J. Adv. Manuf. Technol.* **2016**, *82*, 153–162. [CrossRef]
6. Davies, P.; Johal, A.; Davies, H.; Marchisio, S. Powder interlayer bonding of titanium alloys: Ti-6Al-2Sn-4Zr-6Mo and Ti-6Al-4V. *Int. J. Adv. Manuf. Technol.* **2019**, *103*, 441–452. [CrossRef]
7. Bache, M.R.; Tuppen, S.J.; Voice, W.E.; Lee, H.G.; Aspinwall, D.K. Novel low cost procedure for fabrication of diffusion bonds in Ti 6/4. *Mater. Sci. Technol.* **2009**, *25*, 39–49. [CrossRef]
8. Kah, P.; Suoranta, R.; Martikainen, J.; Magnus, C. Techniques for joining dissimilar materials: Metals and polymers. *Rev. Adv. Mater. Sci.* **2014**, *16*, 229–237.
9. Wulandari, W.; Brooks, G.A.; Rhamdhani, M.A.; Monaghan, B.J. Magnesium: Current and Alternative Production Routes. In Proceedings of the Australian Conference on Chemical Engineering, Hilton Adelaide, Australia, 26–29 September 2010.
10. Akhtar, T.S.; Cooke, K.O.; Khan, T.I.; Shar, M.A. Nanoparticle enhanced eutectic reaction during diffusion brazing of aluminium to magnesium. *Nanomaterials* **2019**, *9*, 370. [CrossRef] [PubMed]

11. Lighweight Materials 2016 Annual Report. Available online: https://www.energy.gov/sites/prod/files/2017/11/f46/FY_2016_APR_Consolidated_Report_compliant-102617.pdf. (accessed on 19 April 2020).
12. Sameer Kumar, D.; Tara Sasanka, C. Magnesium and its alloys. In *Lightweight and Sustainable Materials for Automotive Applications*; Taylor and Francis: Oxfordshire, UK, 2017; ISBN 9781498756884.
13. Wang, M.; Wang, J.; Ke, W. Microelectronics Reliability Corrosion behavior of Sn-3.0Ag-0.5Cu lead-free solder joints. *Microelectron. Reliab.* **2017**, *73*, 69–75. [CrossRef]
14. Ireland, R.; Arronche, L.; Saponara, V. La Electrochemical investigation of galvanic corrosion between aluminum 7075 and glass fiber / epoxy composites modified with carbon nanotubes. *Compos. B. Eng.* **2012**, *43*, 183–194. [CrossRef]
15. Atieh, A.M.; Khan, T.I. TLP bonding of Ti-6Al-4V and Mg-AZ31 alloys using pure Ni electro-deposited coats. *J. Mater. Process. Technol.* **2014**, *214*, 3158–3168. [CrossRef]
16. Atieh, A.M.; Khan, T.I. Effect of process parameters on semi-solid TLP bonding of Ti-6Al-4V to Mg-AZ31. *J. Mater. Sci.* **2013**, *8*, 6737–6745. [CrossRef]
17. Atieh, A.M.; Khan, T.I. Effect of Interlayer Thickness on Joint Formation Between Ti-6Al-4V and Mg-AZ31 Alloys. *J. Mater. Eng. Perform.* **2014**, *23*, 4042–4054. [CrossRef]
18. Shanmugarajan, B.; Padmanabham, G. Fusion welding studies using laser on Ti-SS dissimilar combination. *Opt. Lasers Eng.* **2012**, *50*, 1621–1627. [CrossRef]
19. Cooke, K.O. *Electrodeposited Nanocomposite Coatings: Principles and Applications*; Nova Science Publisher: New York, NY, USA, 2014; Volume 3, ISBN 9781629485690.
20. Tanaka, K.; Nakazawa, T.; Sakairi, K.; Sato, Y.; Kokawa, H.; Omori, T.; Ishida, K. Feasibility of Iridium Containing Nickel Based Superalloy Tool to Friction Stir Spot Welding of High Strength Steel. In *Minerals, Metals and Materials Series*; Springer: Berlin, Germany, 2017.
21. Prangnell, P.B.; Bakavos, D. Novel Approaches to Friction Spot Welding Thin Aluminium Automotive Sheet. In *Materials Science Forum*; Trans Tech Publications Ltd.: Stafa-Zurich, Switzerland, 2010.
22. Simões, S.; Viana, F.; Ramos, A.S.; Teresa Vieira, M.; Vieira, M.F. Microstructural characterization of dissimilar titanium alloys joints using Ni/Al nanolayers. *Metals.* **2018**, *8*, 715. [CrossRef]
23. Cooke, K.O.; Alhazaa, A.; Atieh, A.M. Dissimilar Welding and Joining of Magnesium Alloys: Principles and Application. In *Magnesium—The Wonder Element for Engineering/Biomedical Applications*; Intech: London, UK, 2019.
24. Jalali, A.; Atapour, M.; Shamanian, M.; Vahman, M. Transient liquid phase (TLP) bonding of Ti-6Al-4V/UNS 32750 super duplex stainless steel. *J. Manuf. Process.* **2018**, *33*, 194–202. [CrossRef]
25. Mo, D.F.; Song, T.F.; Fang, Y.J.; Jiang, X.S.; Luo, C.Q.; Simpson, M.D.; Luo, Z.P. A review on diffusion bonding between titanium alloys and stainless steels. *Adv. Mater. Sci. Eng.* **2018**, *2018*, 8701890. [CrossRef]
26. AlHazaa, A.; Alhoweml, I.; Shar, M.A.; Hezam, M.; Abdo, H.S.; AlBrithen, H. Transient liquid phase bonding of Ti-6Al-4V and Mg-AZ31 alloys using Zn coatings. *Materials* **2019**, *12*, 769. [CrossRef]
27. Caiazzo, F.; Curcio, F.; Daurelio, G.; Minutolo, F.M.C. Ti6Al4V sheets lap and butt joints carried out by CO_2 laser: Mechanical and morphological characterization. *J. Mater. Process. Technol.* **2004**, *149*, 546–552. [CrossRef]
28. Balasubramanian, T.S.; Balasubramanian, V.; Muthumanikkam, M.A. Fatigue performance of gas tungsten arc, electron beam, and laser beam welded Ti-6Al-4V alloy joints. *J. Mater. Eng. Perform.* **2011**, *20*, 1620–1630. [CrossRef]
29. Atieh, A.M.; Allaf, R.M.; AlHazaa, A.; Barghash, M.; Mubaydin, H. Effect of Pre- and Post-Weld Shot Peening on the Mechanical and Tribological Properties of TIG Welded Al 6061-T6 Alloy. *Trans. Can. Soc. Mech. Eng.* **2017**, *41*, 197–209. [CrossRef]
30. Habisch, S.; Böhme, M.; Peter, S.; Grund, T.; Mayr, P. The effect of interlayer materials on the joint properties of diffusion-bonded aluminium and magnesium. *Metals.* **2018**, *8*, 138. [CrossRef]
31. Alemán, B.; Gutiérrez, L.; Urcola, J.J. Interface microstructures in diffusion bonding of titanium alloys to stainless and low alloy steels. *Mater. Sci. Technol.* **1993**, *9*, 633–641. [CrossRef]
32. Li, S.; Chen, Y.; Kang, J.; Huang, Y.; Gianetto, J.A.; Yin, L. Interfacial microstructures and mechanical properties of dissimilar titanium alloy and steel friction stir butt-welds. *J. Manuf. Process.* **2019**, *40*, 160–168. [CrossRef]
33. Choi, J.W.; Liu, H.; Ushioda, K.; Fujii, H. Dissimilar friction stir welding of immiscible titanium and magnesium. *Materialia* **2019**, *7*, 100389. [CrossRef]

34. Malikov, A.; Vitoshkin, I.; Orishich, A.; Filippov, A.; Karpov, E. Effect of the aluminum alloy composition (Al-Cu-Li or Al-Mg-Li) on structure and mechanical properties of dissimilar laser welds with the Ti-Al-V alloy. *Opt. Laser Technol.* **2020**, *126*, 106135. [CrossRef]
35. Malikov, A.; Vitoshkin, I.; Orishich, A.; Filippov, A.; Karpov, E. Microstructure and mechanical properties of laser welded joints of Al-Cu-Li and Ti-Al-V alloys. *J. Manuf. Process.* **2020**, *53*, 201–212. [CrossRef]
36. Zhang, Y.; Chen, Y.K.; Zhou, J.P.; Xue, R.L.; Sun, D.Q.; Li, H.M. Characterization of laser beam offset welding of titanium to steel with 38Zn-61Cu alloy filler. *Opt. Laser Technol.* **2020**, *127*, 106195. [CrossRef]
37. Shen, J.; Li, B.; Hu, S.; Zhang, H.; Bu, X. Comparison of single-beam and dual-beam laser welding of Ti–22Al–25Nb/TA15 dissimilar titanium alloys. *Opt. Laser Technol.* **2017**, *93*, 118–126. [CrossRef]
38. Zhang, Y.; Zhou, J.P.; Sun, D.Q.; Gu, X.Y. Nd: YAG laser welding of dissimilar metals of titanium alloy to stainless steel without filler metal based on a hybrid connection mechanism. *J. Mater. Res. Technol.* **2019**, *9*, 1662–1672. [CrossRef]
39. Xu, W.F.; Jun, M.A.; Luo, Y.X.; Fang, Y.X. Microstructure and high-temperature mechanical properties of laser beam welded TC4/TA15 dissimilar titanium alloy joints. *Trans. Nonferrous Met. Soc. China.* **2020**, *30*, 160–170. [CrossRef]
40. Ma, Z.; Jin, Y.; Ji, S.; Meng, X.; Ma, L.; Li, Q. A general strategy for the reliable joining of Al/Ti dissimilar alloys via ultrasonic assisted friction stir welding. *J. Mater. Sci. Technol.* **2019**, *35*, 94–99. [CrossRef]
41. Xiong, X.; Zhao, P.; Ren, R.; Zhang, Z.; Cui, X.; Ji, S. Enhanced resistance-welding hybrid joints of titanium alloy/thermoplastic composites using a carbon-nanotube lamina. *Diam. Relat. Mater.* **2020**, *101*, 107611. [CrossRef]
42. Esfahani Yeganeh, V.; Li, P. Effect of beam offset on microstructure and mechanical properties of dissimilar electron beam welded high temperature titanium alloys. *Mater. Des.* **2017**, *124*, 78–86. [CrossRef]
43. Atieh, A.M.; Khan, T.I. Application of Ni and Cu nanoparticles in transient liquid phase (TLP) bonding of Ti-6Al-4V and Mg-AZ31 alloys. *J. Mater. Sci.* **2014**, *49*, 7648–7658. [CrossRef]
44. Atieh, A.M.; Khan, T.I. Transient liquid phase (TLP) brazing of Mg – AZ31 and Ti – 6Al – 4V using Ni and Cu sandwich foils. *Sci. Technol. Weld. Join.* **2014**, *19*, 333–342. [CrossRef]
45. AlHazaa, A.; Khan, T.I. Diffusion bonding of Al7075 to Ti–6Al–4V using Cu coatings and Sn–3.6Ag–1Cu interlayers. *J. Alloys Compd.* **2010**, *494*, 351–358. [CrossRef]
46. Cooke, K.O. A study of the effect of nanosized particles on transient liquid phase diffusion bonding al6061 metal-matrix composite (MMC) using Ni/Al 2O 3 Nanocomposite Interlayer. *Metall. Mater. Trans. B Process Metall. Mater. Process. Sci.* **2012**, *43*, 627–634. [CrossRef]
47. Gale, W.F.; Butts, D.A. Transient liquid phase bonding. *Sci. Technol. Weld. Join.* **2004**, *9*, 283–300. [CrossRef]
48. Zhuang, W.D.; Eagar, T.W. Transient liquid-phase bonding using coated metal powders. *Weld. J. (Miami, Fla)* **1997**, *76*, 157s.
49. Tuah-Poku, I.; Dollar, M.; Massalski, T. A study of the transient liquid phase bonding process applied to a Ag/Cu/Ag sandwich joint. *Metall. Trans. A Trans. A* **1988**, *19*, 675–686. [CrossRef]
50. Kuntz, M.L.; Zhou, Y.; Corbin, S.F. A study of transient liquid-phase bonding of Ag-Cu using differential scanning calorimetry. *Metall. Mater. Trans. A Phys. Metall. Mater. Sci.* **2006**, *37*, 2493. [CrossRef]
51. Velmurugan, C.; Senthilkumar, V.; Sarala, S.; Arivarasan, J. Low temperature diffusion bonding of Ti-6Al-4V and duplex stainless steel. *J. Mater. Process. Technol.* **2016**, *234*, 272–279. [CrossRef]
52. Kurt, B.; Orhan, N.; Evin, E.; Çalik, A. Diffusion bonding between Ti-6Al-4V alloy and ferritic stainless steel. *Mater. Lett.* **2007**, *61*, 1747–1750. [CrossRef]
53. Balasubramanian, M. Development of processing windows for diffusion bonding of Ti-6Al-4V titanium alloy and 304 stainless steel with silver as intermediate layer. *Trans. Nonferrous Met. Soc. China.* **2015**, *25*, 2932–2938. [CrossRef]
54. Li, H.; Zhang, C.; Liu, H.B.; Li, M.Q. Bonding interface characteristic and shear strength of diffusion bonded Ti-17 titanium alloy. *Trans. Nonferrous Met. Soc. China.* **2015**, *25*, 80–87. [CrossRef]
55. Kenevisi, M.S.; Mousavi Khoie, S.M. An investigation on microstructure and mechanical properties of Al7075 to Ti-6Al-4V Transient Liquid Phase (TLP) bonded joint. *Mater. Des.* **2012**, *38*, 19–25. [CrossRef]
56. Kenevisi, M.S.; Mousavi Khoie, S.M.; Alaei, M. Microstructural evaluation and mechanical properties of the diffusion bonded Al/Ti alloys joint. *Mech. Mater.* **2013**, *64*, 69–75. [CrossRef]

57. Rajakumar, S.; Balasubramanian, V. Diffusion bonding of titanium and AA 7075 aluminum alloy dissimilar joints—process modeling and optimization using desirability approach. *Int. J. Adv. Manuf. Technol.* **2016**, *86*, 1095–1112. [CrossRef]
58. Nakagawa, N.; Hwang, H.Y.; Muller, D.A. Why some interfaces cannot be sharp. *Nat. Mater.* **2006**, *5*, 204–209. [CrossRef]
59. Song, T.F.; Jiang, X.S.; Shao, Z.Y.; Fang, Y.J.; Mo, D.F.; Zhu, D.G.; Zhu, M.H. Microstructure and mechanical properties of vacuum diffusion bonded joints between Ti-6Al-4V titanium alloy and AISI316L stainless steel using Cu/Nb multi-interlayer. *Vacuum* **2017**, *145*, 68–76. [CrossRef]
60. Li, S.X.; Tu, S.T.; Xuan, F.Z. A probabilistic model for prediction of bonding time in diffusion bonding. *Mater. Sci. Eng. A* **2005**, *407*, 250–255. [CrossRef]
61. Zuruzi, A.S.; Li, H.; Dong, G. Effects of surface roughness on the diffusion bonding of Al alloy 6061 in air. *Mater. Sci. Eng. A* **1999**, *270*, 244–248. [CrossRef]
62. Li, B.; Zhang, Z.; Shen, Y.; Hu, W.; Luo, L. Dissimilar friction stir welding of Ti-6Al-4V alloy and aluminum alloy employing a modified butt joint configuration: Influences of process variables on the weld interfaces and tensile properties. *Mater. Des.* **2014**, *53*, 838–848. [CrossRef]
63. Wang, A.; Ohashi, O.; Ueno, K. Effect of surface asperity on diffusion bonding. *Mater. Trans.* **2006**, *47*, 179–184. [CrossRef]
64. Samavatian, M.; Zakipour, S.; Paidar, M. Effect of bonding pressure on microstructure and mechanical properties of Ti-6Al-4V diffusion-bonded joint. *Weld. World* **2017**, *61*, 69–74. [CrossRef]
65. Shirzadi, A.A.; Laik, A.; Tewari, R.; Orsborn, J.; Dey, G.K. Gallium-assisted diffusion bonding of stainless steel to titanium; microstructural evolution and bond strength. *Materialia* **2018**, *4*, 115–126. [CrossRef]
66. Ghosh, M.; Bhanumurthy, K.; Kale, G.B.; Krishnan, J.; Chatterjee, S. Diffusion bonding of titanium to 304 stainless steel. *J. Nucl. Mater.* **2003**, *322*, 235–241. [CrossRef]
67. Simões, S.; Ramos, A.S.; Viana, F.; Vieira, M.T.; Vieira, M.F. Joining of TiAl to steel by diffusion bonding with Ni/Ti reactive multilayers. *Metals.* **2016**, *6*, 96. [CrossRef]
68. Cooke, K.O.; Richardson, A.; Khan, T.I.; Shar, M.A. High-Temperature Diffusion Bonding of Ti–6Al–4V and Super-Duplex Stainless Steel Using a Cu Interlayer Embedded with Alumina Nanoparticles. *J. Manuf. Mater. Process.* **2020**, *4*, 3. [CrossRef]
69. He, P.; Yue, X.; Zhang, J.H. Hot pressing diffusion bonding of a titanium alloy to a stainless steel with an aluminum alloy interlayer. *Mater. Sci. Eng. A* **2008**, *486*, 171–176. [CrossRef]
70. Deng, Y.; Sheng, G.; Yin, L. Impulse pressuring diffusion bonding of titanium to stainless steel using a copper interlayer. *Xiyou Jinshu Cailiao Yu Gongcheng/Rare Met. Mater. Eng.* **2015**, *44*, 1041–1045.
71. Yuan, X.; Liang, X.; Li, X.; Hong, M.; Tang, K. Microstructure and mechanical property of brazed joints in titanium alloy and aluminum alloy combination with tin foil interlayer. *Int. J. Precis. Eng. Manuf.* **2015**, *16*, 1293–1297. [CrossRef]
72. Kundu, S.; Ghosh, M.; Laik, A.; Bhanumurthy, K.; Kale, G.B.; Chatterjee, S. Diffusion bonding of commercially pure titanium to 304 stainless steel using copper interlayer. *Mater. Sci. Eng. A* **2005**, *407*, 154–160. [CrossRef]
73. AlHazaa, A.; Khan, T.I.; Haq, I. Transient liquid phase (TLP) bonding of Al7075 to Ti-6Al-4V alloy. *Mater. Charact.* **2010**, *61*, 312–317. [CrossRef]
74. Kundu, S.; Thirunavukarasu, G.; Chatterjee, S.; Mishra, B. Effect of Bonding Temperature on Phase Transformation of Diffusion-Bonded Joints of Duplex Stainless Steel and Ti-6Al-4V Using Nickel and Copper as Composite Intermediate Metals. *Metall. Mater. Trans. A Phys. Metall. Mater. Sci.* **2015**, *46*, 5756–5771. [CrossRef]
75. Zhang, Z.; Tan, C.; Zhao, X.; Chen, B.; Song, X.; Zhao, H. Influence of Cu coating thickness on interfacial reactions in laser welding-brazing of Mg to Ti. *J. Mater. Process. Technol.* **2018**, *261*, 61–73. [CrossRef]
76. Auwal, S.T.; Ramesh, S.; Zhang, Z.; Yusof, F.; Liu, J.; Tan, C.; Manladan, S.M.; Tarlochan, F. Effect of copper-nickel interlayer thickness on laser welding-brazing of Mg/Ti alloy. *Opt. Laser Technol.* **2019**, *115*, 149–159. [CrossRef]
77. Kundu, S.; Thirunavukarasu, G. Structure and properties correlation of diffusion bonded joint of duplex stainless steel and Ti–6Al–4V with and without Ni–17Cr–9Fe alloy interlayer. *Weld. World* **2016**, *60*, 793–811. [CrossRef]
78. Ferrante, M.; Pigoretti, E.V. Diffusion bonding of Ti-6Al-4V to AISI 316L stainless steel: Mechanical resistance and interface microstructure. *J. Mater. Sci.* **2002**, *37*, 2825–2833. [CrossRef]

79. Akca, E.; Gursel, A. The importance of interlayers in diffusion welding - A review. *Period. Eng. Nat. Sci.* **2015**, *3*, 12–16.
80. Liu, J.; Tan, C.; Wu, L.; Zhao, X.; Zhang, Z.; Chen, B.; Song, X.; Feng, J. Butt laser welding-brazing of AZ31Mg alloy to Cu coated Ti-6Al-4V with AZ92 Mg based filler. *Opt. Laser Technol.* **2019**, *117*, 200–214. [CrossRef]
81. Norouzi, E.; Atapour, M.; Shamanian, M.; Allafchian, A. Effect of bonding temperature on the microstructure and mechanical properties of Ti-6Al-4V to AISI 304 transient liquid phase bonded joint. *Mater. Des.* **2016**, *99*, 543–551. [CrossRef]
82. Simões, S.; Viana, F.; Ventzke, V.; Koçak, M.; Sofia Ramos, A.; Teresa Vieira, M.; Vieira, M.F. Diffusion bonding of TiAl using Ni/Al multilayers. *J. Mater. Sci.* **2010**, *45*, 4351–4357. [CrossRef]
83. Balasubramanian, M. Application of Box-Behnken design for fabrication of titanium alloy and 304 stainless steel joints with silver interlayer by diffusion bonding. *Mater. Des.* **2015**, *77*, 161–169. [CrossRef]
84. Deng, Y.; Sheng, G.; Xu, C. Evaluation of the microstructure and mechanical properties of diffusion bonded joints of titanium to stainless steel with a pure silver interlayer. *Mater. Des.* **2013**, *46*, 84–87. [CrossRef]
85. Afghahi, S.S.S.; Ekrami, A.; Farahany, S.; Jahangiri, A. Fatigue properties of temperature gradient transient liquid phase diffusion bonded Al7075-T6 alloy. *Trans. Nonferrous Met. Soc. China (English Ed.)* **2015**, *25*, 1073–1079. [CrossRef]
86. Li, P.; Li, J.; Xiong, J.; Zhang, F.; Raza, S.H. Diffusion bonding titanium to stainless steel using Nb/Cu/Ni multi-interlayer. *Mater. Charact.* **2012**, *68*, 82–87. [CrossRef]
87. Samavatian, M.; Khodabandeh, A.; Halvaee, A.; Amadeh, A.A. Transient liquid phase bonding of Al 2024 to Ti-6Al-4V alloy using Cu-Zn interlayer. *Trans. Nonferrous Met. Soc. China.* **2015**, *25*, 770–775. [CrossRef]
88. Lee, M.K.; Lee, J.G.; Choi, Y.H.; Kim, D.W.; Rhee, C.K.; Lee, Y.B.; Hong, S.J. Interlayer engineering for dissimilar bonding of titanium to stainless steel. *Mater. Lett.* **2010**, *64*, 1105–1108. [CrossRef]
89. Yuan, X.; Kim, M.B.; Kang, C.Y. Characterization of transient-liquid-phase-bonded joints in a duplex stainless steel with a Ni-Cr-B insert alloy. *Mater. Charact.* **2009**, *60*, 1289–1297. [CrossRef]
90. Kenevisi, M.S.; Mousavi Khoie, S.M. A study on the effect of bonding time on the properties of Al7075 to Ti-6Al-4V diffusion bonded joint. *Mater. Lett.* **2012**, *76*, 144–146. [CrossRef]
91. Anbarzadeh, A.; Sabet, H.; Abbasi, M. Effects of successive-stage Transient Liquid Phase (S-TLP) on microstructure and mechanical properties of Al2024 to Ti-6Al-4V joint. *Mater. Lett.* **2016**, *178*, 280–283. [CrossRef]
92. Chang, S.Y.; Tsao, L.C.; Lei, Y.H.; Mao, S.M.; Huang, C.H. Brazing of 6061 aluminum alloy/Ti-6Al-4V using Al-Si-Cu-Ge filler metals. *J. Mater. Process. Technol.* **2012**, *212*, 8–14. [CrossRef]
93. Kundu, S.; Sam, S.; Chatterjee, S. Evaluation of interface microstructure and mechanical properties of the diffusion bonded joints of Ti-6Al-4V alloy to micro-duplex stainless steel. *Mater. Sci. Eng. A* **2011**, *528*, 4910–4916. [CrossRef]